Research Article

SENP3 Aggravates Renal Tubular Epithelial Cell Apoptosis in Lipopolysaccharide-Induced Acute Kidney Injury via deSUMOylation of Drp1

Lirui Wang   Jiangtao Li   Chen Yu

Department of Nephrology, Tongji Hospital, Tongji University School of Medicine, Shanghai, China

Abstract

Background: Sepsis causes acute kidney injury (AKI) in critically ill patients, although the mechanisms underlying the pathophysiology are not fully understood. SUMO-specific proteases 3 (SENP3), a member of the deSUMOylating enzyme family, is known as a redox sensor and could regulate multiple cellular signaling pathways. However, the role of SENP3 in septic AKI remains unclear. *Objectives:* The purpose of this study was to investigate the role of SENP3 in lipopolysaccharide (LPS)-induced AKI model. *Methods:* C57BL/6 mice were given intraperitoneal injection of LPS (10 mg/kg). NRK-52E cells were treated with LPS in vitro. The SENP3 protein expression was analyzed by Western blotting. The levels of reactive oxygen species (ROS) in cells were measured using DCFH-DA. SENP3-siRNA or SENP3-plasmid was, respectively, transfected into NRK-52E cells to knock down or overexpress the SENP3 expression. Western blotting was performed to analyze the protein expression of cleaved caspase 3, cytochrome c, and dynamin-related protein 1 (Drp1). The mitochondrial membrane potential was measured using JC-1 assay kit. Co-immunoprecipitation was used to determine the interaction of Drp1 and SMUO2/3. *Results:* SENP3 protein expression was obviously increased in renal tissues from the mouse model of LPS-induced AKI. Accordingly, SENP3 expression was upregulated in NRK-52E cells treated with LPS in a ROS-dependent manner in vitro. Knockdown of SENP3 dramatically ameliorated LPS-induced apoptosis of NRK-52E cells, whereas overexpression of SENP3 further aggravated LPS-induced apoptosis of NRK-52E cells. Mechanistically, SENP3 triggered Drp1 recruitment to mitochondria by increasing the deSUMOylation of Drp1. *Conclusion:* SENP3 aggravated renal tubular epithelial cell apoptosis in LPS-induced AKI via Drp1 deSUMOylation manner.

© 2022 The Author(s).
Published by S. Karger AG, Basel

Introduction

Sepsis is defined as life-threatening organ dysfunction caused by a dysregulated host response to infection [1]. Acute kidney injury (AKI) is one of the most common complications of sepsis, which significantly increases the risk of mortality [2]. Patients with sepsis-induced AKI have a remarkably increased mortality compared to patients without AKI [3–5]. It has been reported that approximately 60% of patients with sepsis develop AKI and sepsis is the most common cause of AKI in the intensive care unit [6, 7]. However, there is no effective therapy for

Correspondence to:
Chen Yu, yuchen@tongji.edu.cn

septic AKI, mainly due to the lack of complete understanding of kidney injury pathogenesis in sepsis, calling for a need to further elucidate its molecular mechanism.

The mechanisms underlying the pathophysiology of sepsis-induced AKI are complex and not fully understood, but they may include oxidative stress, mitochondrial dysfunction, and tubule epithelia cell apoptosis [8, 9]. Oxidative stress plays an important role in the development of sepsis-induced AKI and is the major contributor to mitochondrial dysfunction in renal cells after treatment with lipopolysaccharide (LPS) [9]. Tubular epithelial cells are primary targets for acute injury [10] and are susceptible to apoptosis in AKI [11]. Recent studies strongly suggest that mitochondrial fragmentation is a crucial mechanism contributing to tubular damage during AKI [12, 13]. Mitochondria are highly dynamic organelles that maintain their morphology by a delicate balance between two opposing processes, fusion and fission. Mitochondria fission is mainly regulated by dynamin-related protein 1 (Drp1), which is a cytosolic protein that will move to the outer mitochondrial membrane by activation [14].

Small ubiquitin-like modifier (SUMO) proteins express four SUMO paralogs in mammals, including SUMO1, SUMO2, SUMO3, and SUMO4. SUMO modification (SUMOylation), one of the post-translational modifications, has been discovered as a critical regulatory mechanism in multiple signaling pathways that alters the cellular localization, protein-protein interaction, and biological function of target proteins [15]. SUMOylation is a dynamic process that can be reversed by SUMO-specific proteases (SENPs) to maintain the balance between the SUMOylation and deSUMOylation of target proteins [16]. SENPs, composed of six members (SENP1, 2, 3, 5, 6, 7) in mammals, detach the specific SUMO paralogs from target proteins. Generally, SENP1 and SENP2 deconjugate SUMO1 or SUMO2/3, SENP3 and SENP5 have specific activity for SUMO2/3 deconjugation, and SENP6 and SENP7 can edit polySUMO2/3 chains [17, 18]. As a crucial member of the SENPs, SENP3 is a redox-sensitive enzyme and is unique in its rapid increases in protein level following a mild increase in reactive oxygen species (ROS) [19]. Multiple studies have shown that SENP3 is associated with the progression of many diseases, including cardiovascular diseases, neurological diseases, nonalcoholic fatty liver disease and various cancers [15]. However, it remains unknown whether SENP3 is involved in the pathogenesis of sepsis-induced AKI. Thus, the aim of the current study is to explore the role of SENP3 in the progression of LPS-induced AKI.

Materials and Methods

Animal Model
C57BL/6 mice (male, 8 weeks old, 20–24 g) were purchased from the Animal Laboratory Center of Tongji University. All efforts were made to ameliorate the suffering of animals, and this study was approved by the Ethics Committee of Tongji Hospital of Tongji University. Mice were randomly assigned to two groups (*n* = 4–6 animals per group): control (Con) group and LPS group. The Con group was given intraperitoneal injection of saline (0.5 mL), while the LPS group was given intraperitoneal injection of LPS (10 mg/kg; Sigma-Aldrich) in 0.5 mL of saline. Mice were euthanized at 24 h after LPS treatment, and then blood and kidney samples were collected.

Renal Function and Histology Analyses
Blood urea nitrogen (BUN) and serum creatinine (Scr) were measured by analytical kits (Huilin Biotech, Changchun, China) using automatic biochemistry analyzer (Rayto Life and Analytical Sciences, Shenzhen, China). Kidney samples were fixed with paraformaldehyde (4%), then embedded in paraffin, and cut into 4 μm thick sections, which were stained with hematoxylin and eosin. The pathological changes of the stained kidney samples were observed under an optical microscope. To evaluate the renal tubular injury, a semiquantitative scoring method was used. In brief, the score was calculated under ×400 magnification observing ten randomly fields for each mouse. Kidney injury score is scored as 0, normal; 1, <10%; 2, 10–25%; 3, 25–50%; 4, 50–75%; 5, 75–100%. This criterion includes lumen occlusion, loss of brush border, and tubular dilation.

Transmission Electron Microscopy
Renal cortex tissues were fixed with 2.5% glutaraldehyde for 2 h at room temperature and transferred to 4°C for storage. After dehydration in ethanol, the specimens were embedded in EPON. Ultrathin sections were photographed under a Hitachi 7700 transmission electron microscope (Tokyo, Japan).

Cell Culture
Normal rat kidney tubular epithelial cells (NRK-52E) (*Rattus norvegicus*, cell strain) were cultured using high-glucose Dulbecco's Modified Eagle's Medium (HyClone) containing 5% fetal bovine serum (Beyotime, Shanghai, China) under 37°C and 5% CO_2 condition. Then, cells were incubated with the optimum concentration of LPS of the indicated times.

Transfection of siRNA and Plasmid
The SENP3-siRNA, negative Con (NC)-siRNA, SENP3-plasmid, and NC-plasmid (empty vehicle pEX-3) were purchased from GenePharma (Shanghai, China) and were transfected into NRK-52E cells using the Lipo6000™ (Beyotime) according to the manufacturer's instructions. Then, NRK-52E cells were subjected to LPS addition for the indicated times. Next, cells were lysed for protein extraction, and samples were analyzed by Western blotting. The sequences of SENP3-siRNA oligonucleotides were as follows: sense 5′-GGUACUACAGCUGAUCCAATT-3′ and antisense 5′-UUGGAUCAGCUGUAGUACCTT-3′. The full sequence of SENP3-Plasmid was described in the online supplementary information (see www.karger.com/doi/10.1159/000525308 for all online suppl. material).

Western Blotting

Proteins were collected from kidney tissues or NRK-52E cells with RIPA lysis buffer (Beyotime). The protein concentration was determined using the BCA assay kit (Beyotime). The protein (30–50 mg) from each group was separated by using SDS-PAGE and electrophoretically transferred onto PVDF membranes (CAT. NO. ISEQ00010, Immobilon®-P^{SQ}). After transfer, nonspecific binding was prevented using 5% skimmed milk TBS-Tween (BBI Life Sciences). The primary antibodies were used as follows: anti-SENP3 (ab124790), anti-SUMO2/3 (ab109005), anti-Drp1 (ab184247), anti-cytochrome C (ab13575) (Abcam); anti-cleaved caspase-3, anti-COX IV (Cell Signaling Technology); anti-GAP-DH (Proteintech). Membranes were then incubated with HRP-labeled secondary antibodies (1:1,000 dilution) at room temperature for 1 h. Each step described above was followed by three washes for 10 min each. Finally, the signals were detected using the AIC. AIphaView imaging system.

Co-Immunoprecipitation

NRK-52E cells were lysed, the supernatants obtained by centrifuging were incubated with anti-Drp1 (ab184247; Abcam) antibody, or IgG (NC) on a shaker overnight at 4°C, and then protein A + G agarose (Beyotime) were added at 4°C slowly shook for 1–3 h. The beads were then rinsed with PBS and subjected to SDS-PAGE. Protein bands were detected by Western blot using anti-SUMO2/3 (ab109005; Abcam) antibodies.

Detection of Intracellular ROS Levels by Fluorescence Microscopy

The ROS levels in cells were measured using 2′,7′-dichlorofluorescein diacetate (DCFH-DA) (Beyotime). N-acetylcysteine (NAC) (Beyotime), a ROS inhibitor, was pre-treated before LPS administration. Cells were treated with LPS (1 μg/mL) for 24 h. Then, the cells were washed twice with cold PBS, treated with DCFH-DA (10 μM final concentration), and incubated for 30 min at 37°C in a light-protected, humidified chamber. After probe treatment, the cells were washed at least twice with cold PBS. A fluorescence microscope (Nikon) was used at set excitation and emission wavelengths in these experiments.

Mitochondrial and Cytosolic Component Extraction

Mitochondrial and cytosolic protein of renal tissue or NRK-52E cells was extracted using a Tissue Mitochondria Isolation Kit or Cell Mitochondria Isolation Kit (Beyotime). First, renal tissue or NRK-52E cells were well distributed by Mitochondria Isolation

Solution containing PMSF in an ice bath for 15 min. A glass homogenizer was applied to grind the tissue or cells followed by centrifugation with 600 *g* for 10 min at 4°C. The liquid supernatant was shifted to another tube and centrifuged again with 11,000 *g* for 10 min at 4°C. The sediment was blended with Mitochondrial Lysate Solution to obtain mitochondrial proteins. The supernatant was centrifuged with 12,000 *g* for 10 min at 4°C to obtain cytosolic proteins.

Mitochondrial Membrane Potential

The mitochondrial membrane potential (ΔΨm) was measured using mitochondrial membrane potential assay kit with JC-1 (Beyotime) according to the manufacturer's instructions. Briefly, after indicated treatments, NRK-52E cells cultured in 6-well plates were washed by PBS and were incubated with JC-1 working solution for 20 min at 37°C. Then, cells were washed twice with JC-1 staining buffer. JC-1 stained cells were measured using a fluorescence microscope (Nikon).

Statistical Analysis

Data are expressed as means ± SEM. Sample means were compared using *t* tests or one-way ANOVA. Statistical analyses were performed with GraphPad Prism 8 software. A value of *p* < 0.05 was considered statistically significant.

Results

LPS-Induced Mitochondrial Fragmentation and Kidney Injury in Mice

In the current study, sepsis-induced AKI mice model was established by intraperitoneal injecting LPS (10 mg/kg) for 24 h. Saline-injected mice were used as Con group. We observed the morphology of mitochondria in kidney cortices of the two groups' mice by transmission electron microscopy. As shown in Figure 1a, mitochondria in tubular cells of mice in the LPS group had significantly increased fragmentation compared to the Con group. At the molecular level, we evaluated the mainly mitochondrial fission regulating proteins of Drp1 with extracted mito-

Fig. 1. Renal SENP3, mitochondrial fragmentation, and cell apoptosis were increased in mice model of LPS-induced AKI. C57BL/6 mice were randomly assigned to two groups: Con group and LPS group. Mice in the LPS group were treated with LPS intraperitoneal injection (10 mg/kg) for 24 h. Serum and kidney samples were collected from the two groups at 24 h. **a** Representative electron microscopy images of mitochondria in renal cortex from two groups are shown (scale bar, 2 μm). Arrows indicate fragmented mitochondria. **b** Western blotting analysis of Drp1 protein expression in the mitochondrial fraction of renal tissues of two groups. COX IV served as a loading Con for mitochondrial protein. **c** Western blotting analysis of SENP3, cleaved caspase-3, and Drp1 protein expressions in whole homogenate of renal tissue of two groups. **d** Western blotting analysis of cytochrome c expression in the cytosolic fraction of renal tissues in the two groups. Representative Western blots and quantitative data are presented. **e** BUN and Scr levels were determined in the two groups. **f** Representative images of HE-stained kidney sections are shown in two groups (scale bar, 20 μm). Arrows within images show damaged tubules. **g** Quantification of tubular injury was determined for each animal by histology scoring as described in the materials and methods section (*p < 0.05 vs. Con group; n = 4–6). BUN, blood urea nitrogen; Scr, serum creatinine; Con, control; LPS, lipopolysaccharide; HE, hematoxylin and eosin.
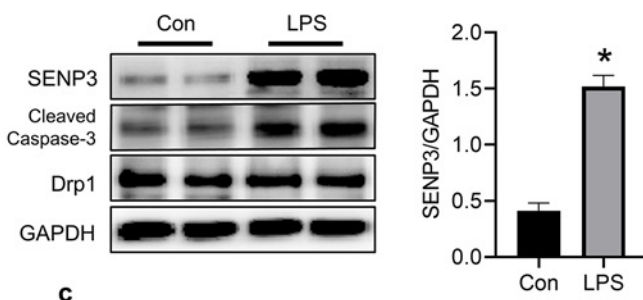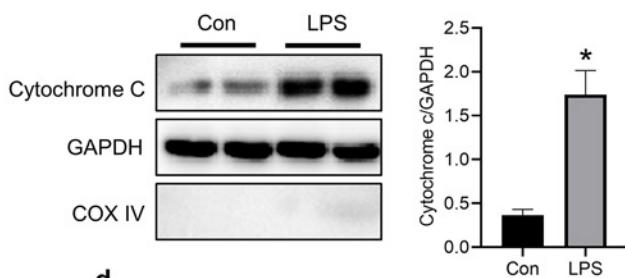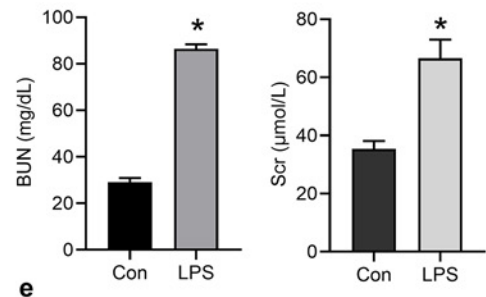
(For figure see next page.)
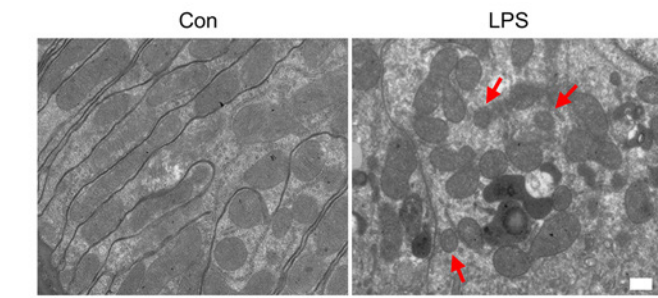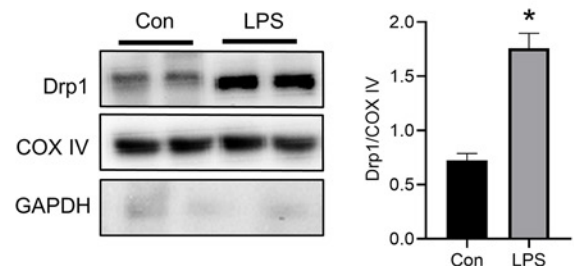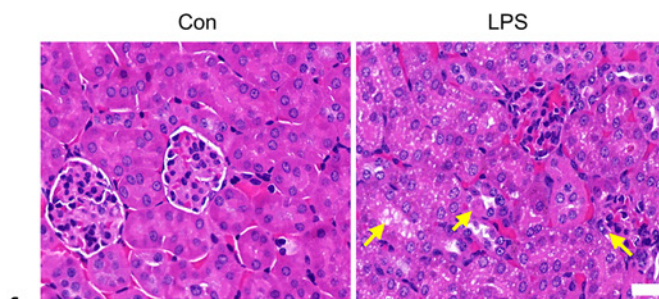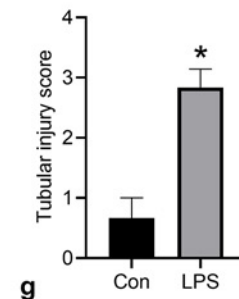
chondrial fractions and whole kidney tissue lysate. We found that mitochondrial Drp1 was increased significantly in the LPS group compared with the Con group (Fig. 1b). No difference of Drp1 was observed in the whole tissue lysates between the two groups (Fig. 1c). Renal tubular cell apoptosis evaluated by Western blotting analysis of cleaved caspase-3 was increased significantly in the LPS group (Fig. 1c). Increased cytochrome c release into the cytosol was observed in the LPS group (Fig. 1d). As shown in Figure 1e, LPS-treated mice exhibited a significant increase in BUN (86.47 ± 1.88 mg/dL vs. 29.07 ± 1.81 mg/dL; $p < 0.05$) and Scr (66.58 ± 6.35 μmol/L vs. 35.34 ± 2.75 μmol/L; $p < 0.05$) compared with the Con group. As shown in Figure 1f, renal histology by H&E staining revealed that LPS-treated mice showed more severe renal tubular damage including lumen occlusion, loss of brush border, and tubular dilation. The tubular injury score of the LPS group was significantly higher than that in the Con group (2.83 ± 0.31 vs. 0.67 ± 0.33; $p < 0.05$; Fig. 1g). Taken together, these data demonstrated that LPS could induce mitochondrial fragmentation, cellular apoptosis, and AKI in vivo.

SENP3 Protein Expression Was Upregulated in LPS-Induced AKI Model in vivo and in vitro

To investigate the potential roles of SENP3 in LPS-induced AKI, we first examined SENP3 expression in the kidney tissue of mice with or without LPS injection. As shown in Figure 1c, Western blotting showed that the renal SENP3 protein expression was significantly increased at 24 h after LPS injection.

And then, to determine the SENP3 expression in LPS-induced AKI model in vitro, SENP3 protein levels were examined using Western blotting in NRK-52E cells stimulated with different concentrations or time of LPS. Figure 2a shows the SENP3 levels in NRK-52E cells stimulated with different concentrations of LPS 0, 0.2, 1, 2, 5, or 10 μg/mL. Figure 2b shows the levels of SENP3 in cells treated with LPS (1 μg/mL) for 6, 12, and 24 h. Thus, LPS dramatically increased the levels of the SENP3 protein partly in a dose- and time-dependent manner.

Since SENP3 was known as a redox sensor responding to ROS accumulation, we investigated whether ROS was responsible for the upregulated SENP3 in LPS-induced AKI. To this end, we suppressed ROS accumulation in LPS-treated NRK-52E cells by pre-treatment of ROS inhibitors NAC (Fig. 2c). We observed that the upregulation of SENP3 was significantly suppressed by NAC in LPS-induced NRK-52E cells (Fig. 2d). These data suggested that SENP3 protein was upregulated in a ROS-dependent manner in LPS-treated NRK-52E cells.

Knockdown of SENP3 Alleviated LPS-Induced Apoptosis of NRK-52E Cells

To further investigate the direct roles of SENP3 in LPS-induced tubular cell apoptosis, we transfected NRK-52E cells with SENP3-siRNA or NC-siRNA and then incubated in the absence or presence of LPS (1 μg/mL) for 24 h. Figure 3a shows that SENP3-siRNA markedly decreased SENP3 protein compared with NC-siRNA, and the levels of SENP3 were lower in SENP3-deficient NRK-52E cells following LPS addition. The apoptotic marker-cleaved caspase-3 was determined. As shown in Figure 3b, cleaved caspase-3 was induced by LPS and reversed by SENP3-siRNA.

Cytochrome c release from mitochondria to cytoplasm is a hallmark of the intrinsic pathway of cell apoptosis [20]. After LPS administration, the amount of cytochrome c in cytoplasm was significantly increased compared to Con group (Fig. 3c). However, the cytochrome c in the cytoplasm was significantly decreased in SENP3-siRNA + LPS group than that in the LPS group (Fig. 3c).

The decrease of ΔΨm is a landmark event in the early stages of cell apoptosis. JC-1 staining was used to measure ΔΨm of NRK-52E cells. JC-1 is a monomer present in the cytoplasm (which stains green), and it also accumulates as aggregates in normally polarized mitochondria (which stains red). A shift in fluorescence from red to green indicates the decreased membrane potential. As shown in Figure 3d, LPS induced mitochondrial depolarization of NRK-52E cells, as evidenced by diffuse cytoplasmic JC-1 green staining. Knockdown of SENP3 using SENP3-siRNA restored mitochondrial membrane potential in LPS-induced NRK-52E cells. These results demonstrated that knockdown of SENP3 alleviated LPS-induced apoptosis of NRK-52E cells.

Overexpression of SENP3 Further Aggravated LPS-Induced Apoptosis of NRK-52E Cells

NRK-52E cells were transfected with SENP3-plasmid or NC-plasmid and then treated with the absence or presence of LPS (1 μg/mL) for 24 h. Figure 4a shows that the SENP3 protein was remarkably increased in the SENP3-plasmid group compared with the NC-plasmid group, and the levels of SENP3 were further higher in SENP3-overexpression NRK-52E cells following LPS addition. As shown in Figure 4b, the apoptotic marker-cleaved caspase-3 was significantly increased in SENP3-plasmid + LPS groups compared with the NC-plasmid + LPS groups. Figure 4c shows that the amount of cytochrome c in cytoplasm in the SENP3-plasmid + LPS
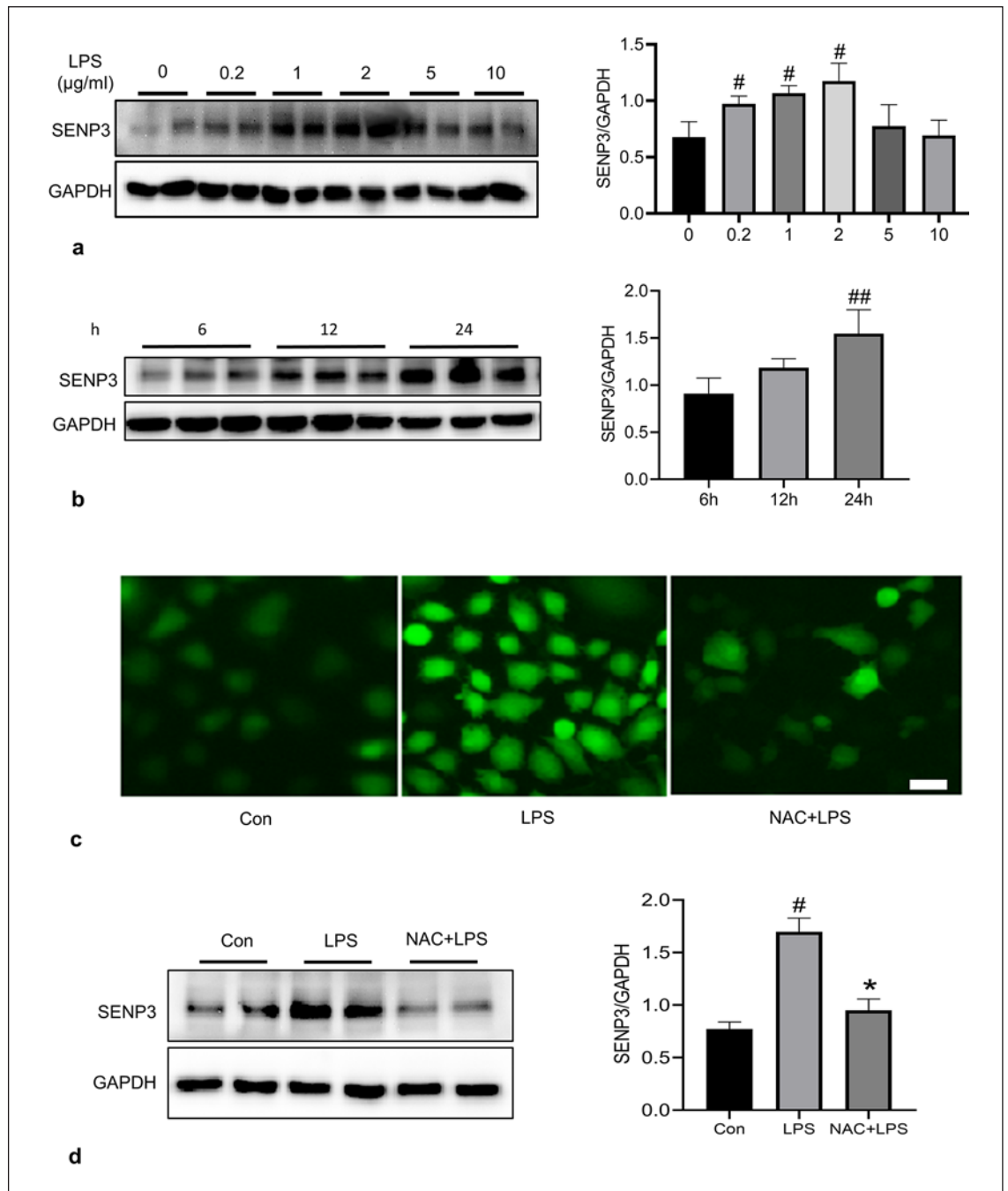
Fig. 2. SENP3 protein expression was upregulated in NRK-52E cells treated with LPS by ROS production. **a** NRK-52E cells were treated with different doses of LPS for 24 h. SENP3 expression was measured using Western blotting ($n = 4$, $^{#}p < 0.05$ vs. 0 μg/mL group). **b** NRK-52E cells were treated with LPS (1 μg/mL) for different times. SENP3 expression was measured using Western blotting ($n = 3$, $^{##}p < 0.05$ vs. 6 h group). **c** DCFH-DA was used to detect ROS production in NRK-52E cells treated with LPS or NAC + LPS (scale bars, 100 μm). **d** SENP3 protein expression in NRK-52E cells treated with LPS or NAC + LPS was measured using Western blotting ($^{#}p < 0.05$ vs. Con group; $^{*}p < 0.05$ vs. LPS group; $n = 4$).
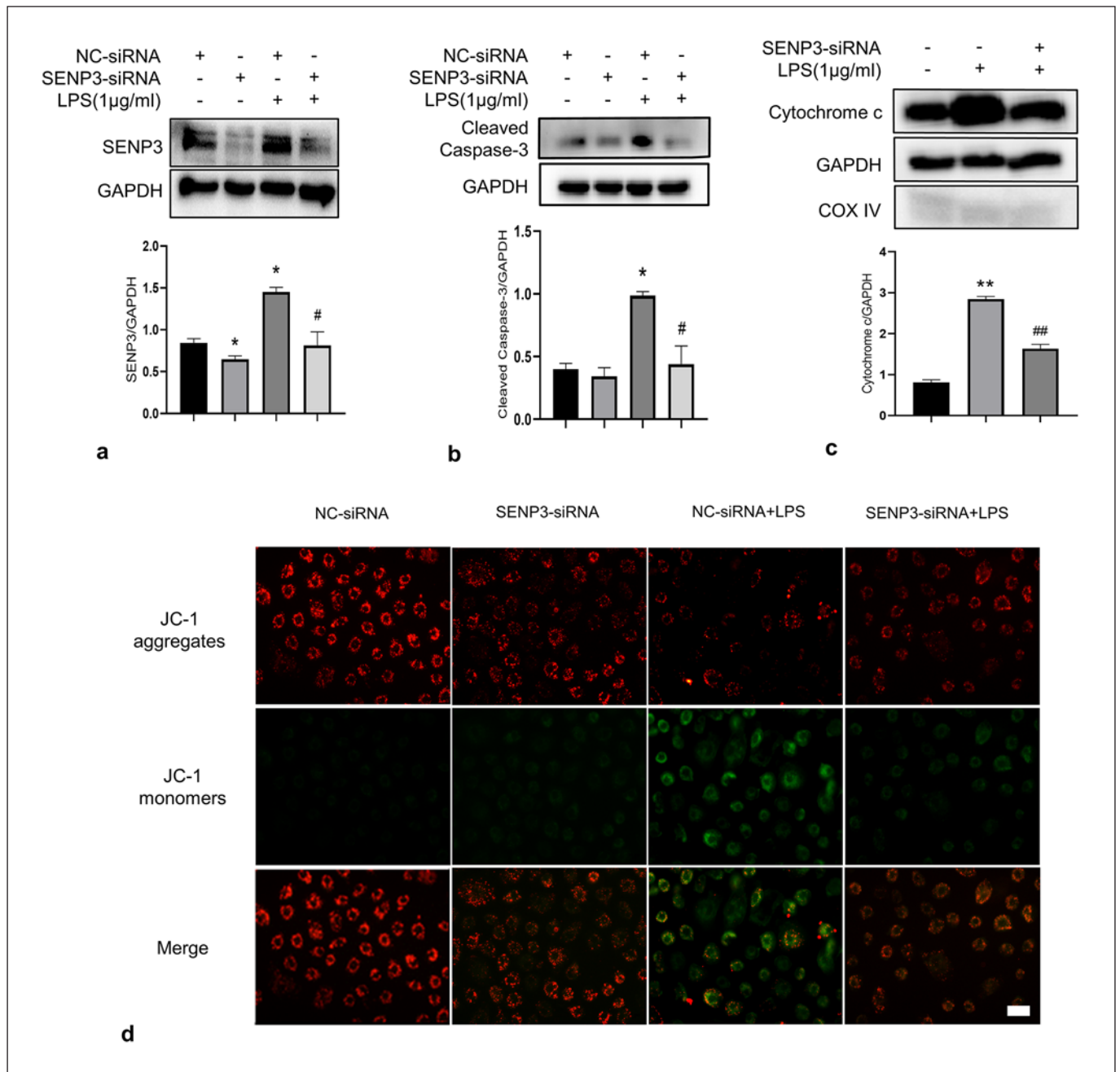
Fig. 3. Knockdown of SENP3 alleviated LPS-induced apoptosis of NRK-52E cells. NRK-52E cells were transfected with SENP3-siRNA or NC-siRNA and then incubated in the absence or presence of LPS (1 μg/mL) for 24 h. **a** Western blotting was used to analyze the levels of the SENP3 in NRK-52E cells. **b** Western blotting for the apoptosis-related protein cleaved caspase-3 in NRK-52E cells. **c** Western blotting analysis of the amount of cytochrome c in the cytosol of NRK-52E cells. Representative Western blots and quantitative data are presented. **d** JC-1 staining was used to analyze mitochondrial membrane potential of NRK-52E cells. Red fluorescence and green fluorescence represent JC-1 aggregates and JC-1 monomers, respectively (scale bars, 100 μm) (*$p < 0.05$ vs. NC-siRNA group; #$p < 0.05$ vs. NC-siRNA + LPS group; **$p < 0.05$ vs. Con group; ##$p < 0.05$ vs. LPS group; $n = 3$).
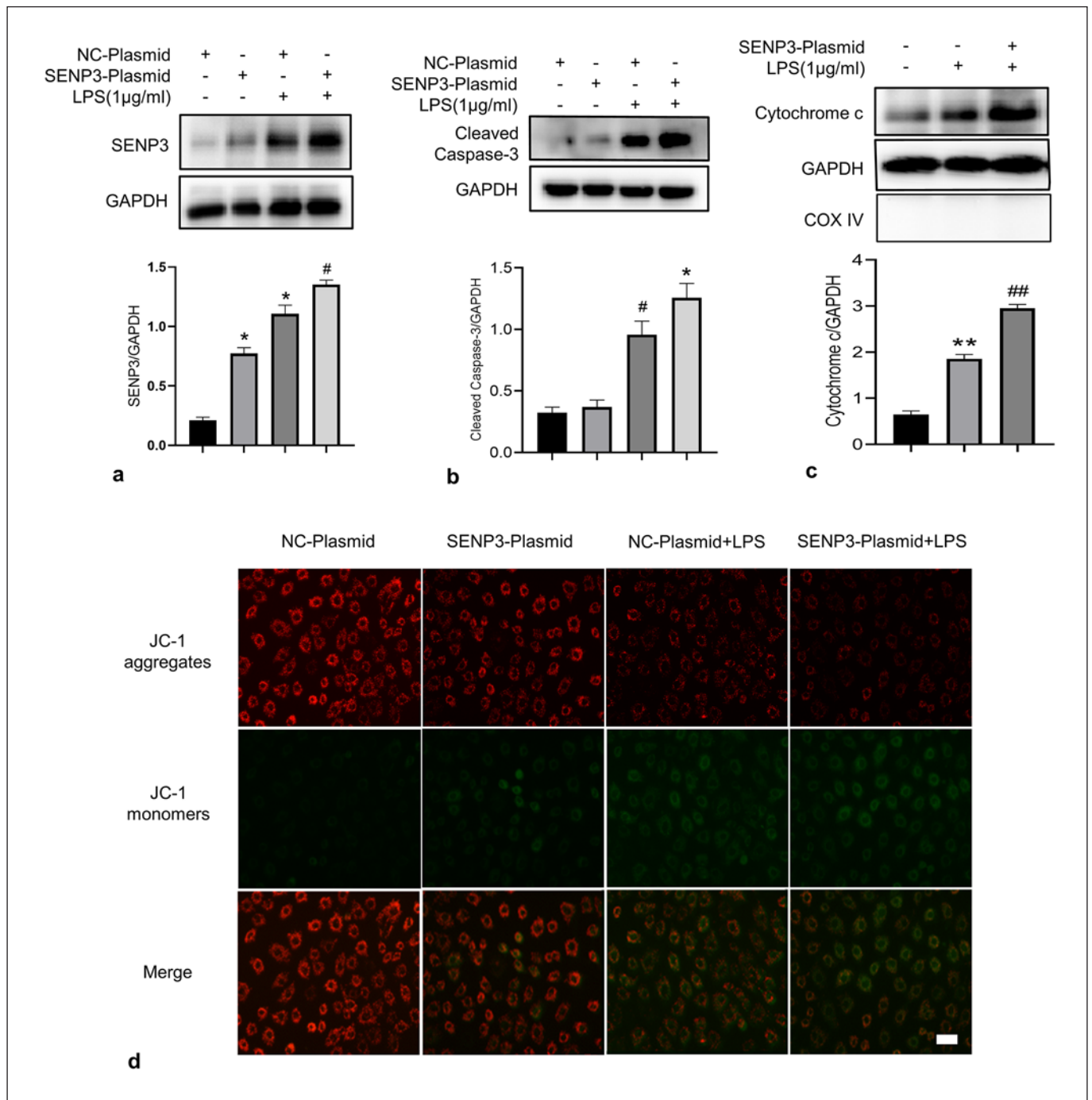
Fig. 4. Overexpression of SENP3 further aggravated LPS-induced apoptosis of NRK-52E cells. NRK-52E cells were transfected with SENP3-plasmid or NC-plasmid and then incubated in the absence or presence of LPS (1 μg/mL) for 24 h. **a** Western blotting was used to analyze the levels of the SENP3 in NRK-52E cells. **b** Western blotting for the apoptosis-related protein cleaved caspase-3 in NRK-52E cells. **c** Western blotting analysis of the amount of cyto-chrome c in the cytosol of NRK-52E cells. Representative Western blots and quantitative data are presented. **d** JC-1 staining was used to analyze mitochondrial membrane potential of NRK-52E cells. Red fluorescence and green fluorescence represent JC-1 aggregates and JC-1 monomers, respectively (scale bars, 100 μm) (*$p < 0.05$ vs. NC-plasmid group; #$p < 0.05$ vs. NC-plasmid + LPS group; **$p < 0.05$ vs. Con group; ##$p < 0.05$ vs. LPS group; $n = 3$).
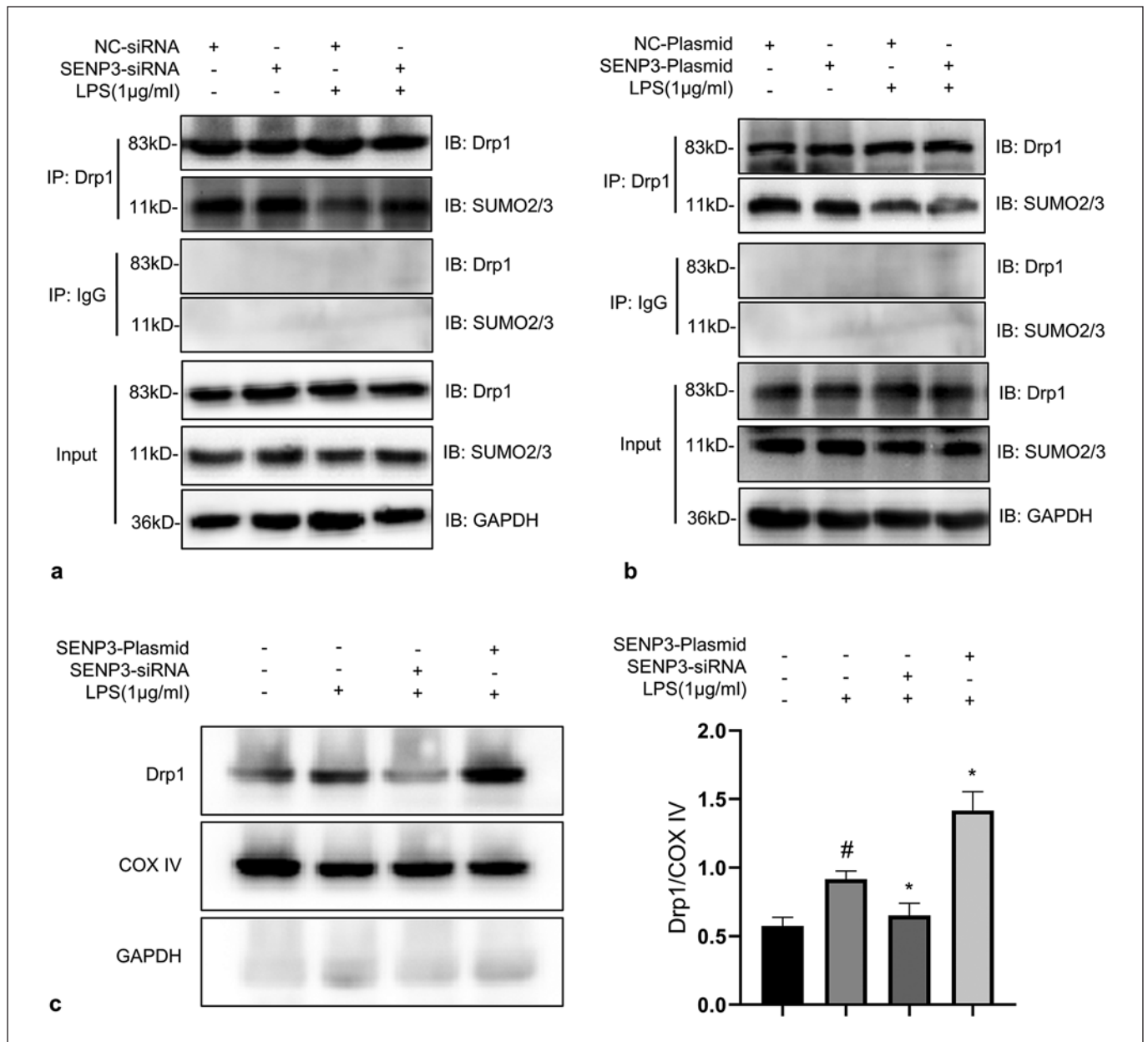
Fig. 5. SENP3 promoted deSUMOylation of Drp1 and facilitated Drp1 translocation to mitochondria. **a**, **b** NRK-52E cells were transfected with SENP3-siRNA/NC-siRNA (**a**) (or SENP3-plasmid/NC-plasmid (**b**)) and then incubated in the absence or presence of LPS (1 μg/mL) for 24 h. The interaction of Drp1 with SMUO2/3 was determined by co-IP. Whole-cell lysates were used for pull-down assay. IP was performed with Drp1 antibody or IgG, and immunoblotting (IB) was performed with SUMO2/3 and Drp1 antibodies. **c** The expression of Drp1 protein in mitochondrial fraction was evaluated using Western blotting analysis. COX IV served as a loading Con for mitochondrial protein. Representative Western blots and quantitative data are presented (*$p < 0.05$ vs. LPS group; #$p < 0.05$ vs. con group; $n = 3$).

groups was further increased relative to the LPS groups. Overexpression of SENP3 further decreased mitochondrial membrane potential in LPS-induced NRK-52E cells

(Fig. 4d). These data indicated that overexpression of SENP3 further aggravated LPS-induced apoptosis of NRK-52E cells.
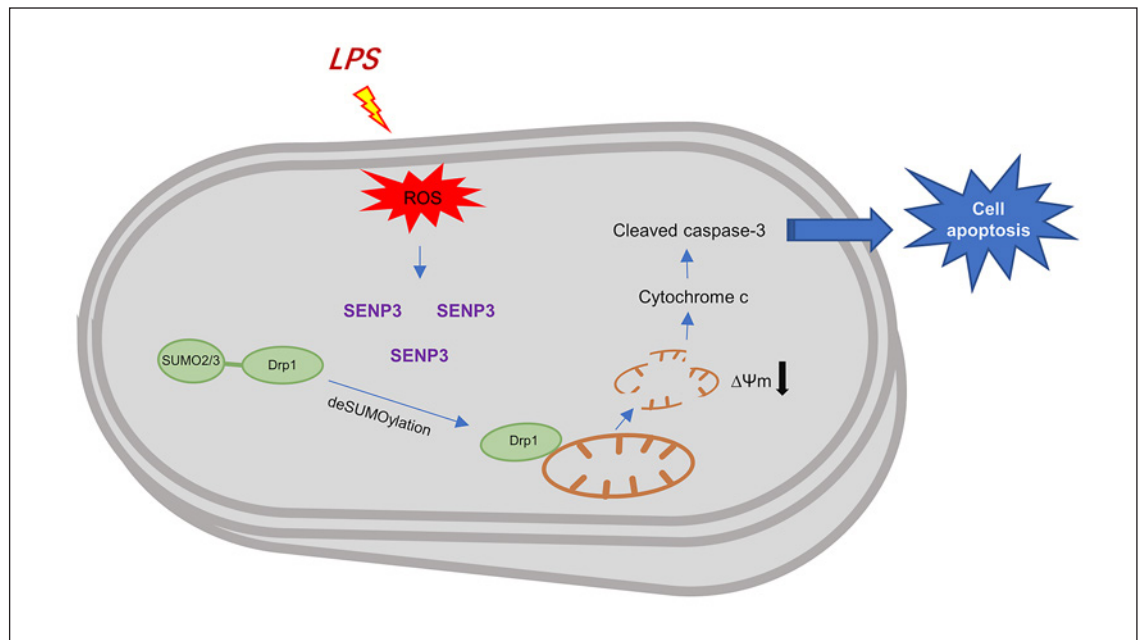
Fig. 6. A schematic model of SENP3 function in LPS-induced AKI signaling.

SENP3 Promoted deSUMOylation of Drp1 and Facilitated Drp1 Translocation to Mitochondria

Our forementioned results demonstrated that SENP3 played a detrimental role of LPS-induced AKI. To further gain insight into the underlying molecular mechanism mediating the pathological effects of SENP3, we detected the effect of SENP3 on Drp1. Co-IP method was used to detect the interaction between Drp1 and SUMO2/3, and this result indicated that Drp1 can be SUMOylated by SUMO2/3 (Fig. 5a, b). LPS exposure decreased the conjugation between SUMO2/3 and Drp1, and this decrease was further enhanced after transfected with SENP3-plasmid (Fig. 5b) and however transfected with SENP3-siRNA restored the conjugation between SUMO2/3 and Drp1 (Fig. 5a). As shown in Figure 5c, mitochondrial Drp1 expression was significantly increased in LPS-treated NRK-52E cells, which was significantly suppressed by SENP3 silencing while further augmented by SENP3 overexpression. These results demonstrated that SENP3 promoted deSUMOylation of Drp1 and facilitated Drp1 translocation to mitochondria in LPS-treated NRK-52E cells.

Discussion

Increased understanding of the mechanisms underlying the physiopathology of LPS-induced AKI is important for the identification of novel therapeutic targets. In the present study, we provided new insights into the role of SENP3 in LPS-induced AKI. First, we found that the expression of SENP3 was upregulated in LPS-induced AKI model in vivo and in vitro. Second, knockdown of SENP3 alleviated LPS-induced apoptosis of NRK-52E cells, whereas overexpression of SENP3 further aggravated LPS-induced apoptosis of NRK-52E cells, indicating a negative role of SENP3 in the setting of LPS-induced AKI. Mechanistic studies indicated that SENP3 promoted LPS-induced apoptosis mainly via deSUMOylation of Drp1-mediated mitochondrial fission (Fig. 6).

Previous studies have demonstrated that SENP3 is widely expressed in various organ and cell types and is upregulated in multiple disease conditions largely in a ROS-dependent manner. It has been reported that SENP3 was expressed and upregulated in the mouse heart depending on ROS production in response to myocardial ischemia-reperfusion (MIR) injury [21]. Hepatic SENP3 was upregulated in nonalcoholic fatty liver disease patients and an animal model in vivo and after load-

ing hepatocytes with free fatty acids in vitro [22]. SENP3 expression was obvious upregulation in the brain after traumatic brain injury, especially in the neurons [23]. SENP3 was highly expressed in vascular smooth muscle cells of remodeled arteries, accompanied by elevated ROS levels [24]. SENP3 mRNA and protein levels were significantly increased in high-glucose cultured human aortic endothelial cells in a time-dependent manner [25]. There was an increase in ROS level and SENP3 expression in Dex-induced osteoporotic BM-MSCs [26]. However, there are few studies concerning the expression of SENP3 in kidney injury. In the current study, we demonstrated that SENP3 was expressed in the mouse kidney tissue and was remarkably upregulated in the mouse kidney tissue in LPS-induced AKI model. In addition, our in vitro findings also suggest that SENP3 was remarkably upregulated depending on ROS accumulation in NRK-52E cells following LPS treatment. It is shown that SENP3 elevation in pathological stress conditions is not organ-specific.

To further investigate the role of SENP3 in LPS-induced AKI, we developed a model in vitro using NRK-52E cells exposed to LPS. Our study found that knockdown of SENP3 reversed LPS-induced increases in cleaved caspase 3, cytochrome c in cytosol, and lower $\Delta\Psi m$ of NRK-52E cells. By contrast, overexpression of SENP3 further aggravated LPS-induced apoptosis of NRK-52E cells, indicating a negative role of SENP3 in the setting of LPS-induced AKI. In other words, our study suggested that SENP3 exerted deleterious effects on cells, which are consistent with previous studies. It has been reported that SENP3 upregulation pivotally contributes to MIR injury [21]. SENP3 overexpression significantly promoted, and sh-RNA-mediated knockdown markedly inhibited vascular smooth muscle cells proliferation and migration [24]. SENP3 was involved in high-glucose-induced endothelial dysfunction [25]. Enhanced adipogenesis and weakened osteogenesis in osteoporotic BM-MSCs might be caused by upregulated SENP3 [26]. However, whether SENP3 promotes cell death or cell survival remains controversial. Some studies have reported a protective effect. For example, knockdown of SENP3 promoted apoptosis after ischemia-reperfusion, indicating the protective role of the SENP3 in MIR injury [27].

Mitochondria are abundant in the kidney and represent the powerhouses of the renal tubular epithelial cells. Mitochondrial dysfunction has been increasingly recognized as a key contributor to the pathogenesis of kidney injure. Drp1 is a GTPase recruited over the mitochon-drial surface upon activation to initiate fission and pivotally mediates mitochondria-dependent apoptosis [14]. Here, our results demonstrated that knockdown of SENP3 reversed Drp1 recruited over mitochondrial in NRK-52E cells treated by LPS, whereas overexpression of SENP3 significantly augmented Drp1 localization at mitochondria. Subsequently, our findings demonstrate that Drp1 was the deSUMOylation target of SENP3. These data suggest that Drp1 might mediate the detrimental effects of SENP3 overexpression on mitochondrial dysfunction and subsequent injury. Consistent with our findings, it has been reported that SENP3 promoted Drp1 mitochondrial translocation in reoxygenated neurons, leading to augmented neural apoptosis [28]. It has also been shown that Drp1 is the major SENP3 target mediating its effects in cardiomyocytes [21]. Collectively, our results provide clues that SENP3-mediating Drp1 deSUMOylation signaling may represent a potential pathway in the mitochondrial damage and kidney injury in LPS-induced AKI.

In summary, SENP3 was upregulated in LPS-induced AKI model in vivo and in vitro. SENP3-mediated deSUMOylation of Drp1 promoted mitochondrial fission and aggravated renal tubular epithelial cell apoptosis in LPS-induced AKI. Such data might shed new light on the pathogenesis of LPS-induced AKI, which may be used as a potential therapeutic target for treatment of sepsis-associated AKI. The precise role of SENP3 in the development of septic AKI will continue to be studied.

Statement of Ethics

All animal experiments were performed under animal study protocols approved by the Ethics Committee of Tongji Hospital of Tongji University (No. 2019-DW-001).

Conflict of Interest Statement

The authors declare that they have no competing interests.

Funding Sources

Wang/Li/Yu

Author Contributions

Lirui Wang: study design, experiments, data analysis, manuscript preparation, and drafting the article. Jiangtao Li and Chen Yu: study design and revising the article.

Data Availability Statement

The data that support the findings of this study are available from the corresponding author on reasonable request.

References

1 Singer M, Deutschman CS, Seymour CW, Shankar-Hari M, Annane D, Bauer M, et al. The Third International consensus definitions for sepsis and septic shock (Sepsis-3). JAMA. 2016 Feb;315(8):801–10.

2 Zarjou A, Agarwal A. Sepsis and acute kidney injury. J Am Soc Nephrol. 2011 Jun;22(6): 999–1006.

3 Yegenaga I, Hoste E, Van Biesen VW, Vanholder R, Benoit D, Kantarci G, et al. Clinical characteristics of patients developing ARF due to sepsis/systemic inflammatory response syndrome: results of a prospective study. Am J Kidney Dis. 2004 May;43(5):817–24.

4 Bagshaw SM, Uchino S, Bellomo R, Morimatsu H, Morgera S, Schetz M, et al. Septic acute kidney injury in critically ill patients: clinical characteristics and outcomes. Clin J Am Soc Nephrol. 2007 May;2(3):431–9.

5 Bouchard J, Acharya A, Cerda J, Maccariello ER, Madarasu RC, Tolwani AJ, et al. A Prospective International Multicenter Study of AKI in the intensive care unit. Clin J Am Soc Nephrol. 2015 Aug;10(8):1324–31.

6 Schrier RW, Wang W. Acute renal failure and sepsis. N Engl J Med. 2004 Jul;351(2):159–69.

7 Bellomo R, Kellum JA, Ronco C, Wald R, Martensson J, Maiden M, et al. Acute kidney injury in sepsis. Intensive Care Med. 2017 Jun;43(6):816–28.

8 Galley HF. Oxidative stress and mitochondrial dysfunction in sepsis. Br J Anaesth. 2011 Jul;107(1):57–64.

9 Quoilin C, Mouithys-Mickalad A, Lécart S, Fontaine-Aupart MP, Hoebeke M. Evidence of oxidative stress and mitochondrial respiratory chain dysfunction in an in vitro model of sepsis-induced kidney injury. Biochim Biophys Acta. 2014 Oct;1837(10):1790–800.

10 Chevalier RL. The proximal tubule is the primary target of injury and progression of kidney disease: role of the glomerulotubular junction. Am J Physiol Renal Physiol. 2016 Jul;311(1):F145–61.

11 Agarwal A, Dong Z, Harris R, Murray P, Parikh SM, Rosner MH, et al. Cellular and molecular mechanisms of AKI. J Am Soc Nephrol. 2016 May;27(5):1288–99.

12 Brooks C, Wei Q, Cho SG, Dong Z. Regulation of mitochondrial dynamics in acute kidney injury in cell culture and rodent models. J Clin Invest. 2009 May;119(5):1275–85.

13 Bhargava P, Schnellmann RG. Mitochondrial energetics in the kidney. Nat Rev Nephrol. 2017 Oct;13(10):629–46.

14 Sumida M, Doi K, Ogasawara E, Yamashita T, Hamasaki Y, Kariya T, et al. Regulation of mitochondrial dynamics by dynamin-related protein-1 in acute cardiorenal syndrome. J Am Soc Nephrol. 2015 Oct;26(10):2378–87.

15 Long X, Zhao B, Lu W, Chen X, Yang X, Huang J, et al. The critical roles of the SUMO-specific protease SENP3 in human diseases and clinical implications. Front Physiol. 2020 Oct;11:558220.

16 Yeh ET. SUMOylation and De-SUMOylation: wrestling with life's processes. J Biol Chem. 2009 Mar;284(13):8223–7.

17 Shen LN, Geoffroy MC, Jaffray EG, Hay RT. Characterization of SENP7, a SUMO-2/3-specific isopeptidase. Biochem J. 2009 Jun; 421(2):223–30.

18 Békés M, Prudden J, Srikumar T, Raught B, Boddy MN, Salvesen GS. The dynamics and mechanism of SUMO chain deconjugation by SUMO-specific proteases. J Biol Chem. 2011 Mar;286(12):10238–47.

19 Lao Y, Yang K, Wang Z, Sun X, Zou Q, Yu X, et al. DeSUMOylation of MKK7 kinase by the SUMO2/3 protease SENP3 potentiates lipopolysaccharide-induced inflammatory signaling in macrophages. J Biol Chem. 2018 Mar;293(11):3965–80.

20 Hall AM, Schuh CD. Mitochondria as therapeutic targets in acute kidney injury. Curr Opin Nephrol Hypertens. 2016 Jul;25(4): 355–62.

21 Gao L, Zhao Y, He J, Yan Y, Xu L, Lin N, et al. The desumoylating enzyme sentrin-specific protease 3 contributes to myocardial ischemia reperfusion injury. J Genet Genomics. 2018 Mar;45(3):125–35.

22 Liu Y, Yu F, Han Y, Li Q, Cao Z, Xiang X, et al. SUMO-specific protease 3 is a key regulator for hepatic lipid metabolism in non-alcoholic fatty liver disease. Sci Rep. 2016 Nov;6: 37351.

23 Yu Z, Li H, Yan HY, Yang YQ, Zhang DD, Huang LT, et al. Expression and cell distribution of SENP3 in brain tissue after traumatic brain injury in mice: a Pilot Study. Cell Mol Neurobiol. 2015 Jul;35(5):733–40.

24 Cai Z, Wang Z, Yuan R, Cui M, Lao Y, Wang Y, et al. Redox-sensitive enzyme SENP3 mediates vascular remodeling via de-SUMOylation of β-catenin and regulation of its stability. EBioMedicine. 2021 May;67:103386.

25 Chen F, Ma D, Li A. SENP3 regulates high glucose-induced endothelial dysfunction via ROS dependent signaling. Diab Vasc Dis Res. 2020;17(6):1479164120970895.

26 Zhang YX, Chen Y, Sun HX, Zhang WK, Zhang LL, Li HY, et al. SENP3-mediated PPARγ2 DeSUMOylation in BM-MSCs potentiates glucocorticoid-induced osteoporosis by promoting adipogenesis and weakening osteogenesis. Front Cell Dev Biol. 2021 Jun;9: 693079.

27 Rawlings N, Lee L, Nakamura Y, Wilkinson KA, Henley JM. Protective role of the deSUMOylating enzyme SENP3 in myocardial ischemia-reperfusion injury. PLoS One. 2019 Apr;14(4):e0213331.

28 Guo C, Hildick KL, Luo J, Dearden L, Wilkinson KA, Henley JM. SENP3-mediated deSUMOylation of dynamin-related protein 1 promotes cell death following ischaemia. EMBO J. 2013 May;32(11):1514–28.